# A Globally Stable High-Performance Adaptive Robust Control Algorithm With Input Saturation for Precision Motion Control of Linear Motor Drive Systems

Yun Hong and Bin Yao

***Abstract*—This paper focuses on the synthesis of nonlinear adaptive robust controller with saturated actuator authority for a linear motor drive system, which is subject to parametric uncertainties and uncertain nonlinearities such as input disturbances as well. Global stability with limited control efforts is achieved by breaking down the overall uncertainties to state-linearly-dependent uncertainties (such as viscous friction) and bounded nonlinearities (such as Coulomb friction, cogging force, etc.), and dealing with them via different strategies. Furthermore, a guaranteed transient performance and final tracking accuracy can be obtained by incorporating the well-developed adaptive robust control strategy and effective parameter identifier. Asymptotic output tracking is also achieved in the presence of parametric uncertainties only. Meanwhile, in contrast to the existing saturated control structures that are designed based on a set of transformed coordinates, the proposed saturated controller is carried out in the actual system states, which have clear physical meanings. This makes it much easier and less conservative to select the design parameters to meet the dual objective of achieving global stability with limited control efforts for rare emergency cases and the local high-bandwidth control for high performance under normal running conditions. Real-time experimental results are obtained to illustrate the effectiveness of the proposed saturated adaptive robust control strategy.**

***Index Terms*—Adaptive control, input saturation, linear motors, motion control, nonlinear systems, robust control.**

## I. Introduction

ALL actuators of physical devices are subject to amplitude saturation. Although, in some applications, it may be possible to ignore this fact, the reliable operation and acceptable performance of most control systems must be assessed in light of actuator saturation [1]. Significant amount of research has been done to stabilize the system while taking into account the saturation nonlinearities at the controller design stage. It was proved in [2] that global stabilization is not possible using linear feedback laws for general linear systems subject to input saturation. A low-and-high gain method was used in [3] and [4] to provide semiglobal stability as well as meeting performance such as disturbance rejection, robustness, and so on for asymptotically null controllable linear systems. For the same class of systems, robust control techniques such as H-infinity was employed in [5] to achieve global stability but with the difficulty to obtain a closed-form expression of the solution for high-dimensional systems. A novel saturated control structure was proposed in [6] to ensure the globally asymptotic stability for a chain of integrators of arbitrary order by intelligently using a set of linear coordinate transformations and multiple saturation-type functions such as sigmoidal functions.

In all those works, it was assumed that the systems of concern are linear and exactly known, which is not the case for most physical systems in reality. Some nonlinear factors such as friction affect system behavior significantly and are rather difficulty to model precisely. There are always discrepancies between the model for controller design and the actual physical system. It is not unusual that some of the system parameters are unknown or their values may vary from time to time. Unpredictable external disturbances also affect the system performance. Therefore, it is of practical importance to take these issues into account when attacking the actuator saturation problem. Gong and Yao [7] combined the wise use of saturation functions proposed in [6] with the adaptive robust control (ARC) strategy proposed in [8] and [9] to achieve both global stability and high performance for a chain of integrators subject to matched parametric uncertainty and uncertain nonlinearities. However, like the saturated controller in [6], the design is based on a set of transformed coordinates, in which the effect of model uncertainties immediately shows up at the beginning step of the backstepping-like controller design, even though the model uncertainties studied are matched uncertainties. In other words, the actual model uncertainties have been "amplified" $n$ times for the control input to accommodate, where $n$ represents the order of the system. Thus, with a limited control authority, the extent of model uncertainties that the resulting controller can handle is very much restricted, leading to a conservative overall design.

In this paper, a new saturated control structure based on the backstepping design [12] and the ARC strategy [8], [9] is proposed. It has been shown in [13] that the proposed ARC [8], [9] can achieve high tracking accuracy (the same level as the

Manuscript received March 1, 2006; revised November 20, 2006. Recommended by Technical Editor Y. Hori. This work was supported in part by the National Science Foundation under Grant CMS-0600516 and in part by the National Natural Science Foundation of China (NSFC) under the Joint Research Fund for Overseas Chinese Young Scholars under Grant 50528505. An earlier version of this paper was presented at the 2005 IEEE/ASME International Conference on Advanced Intelligent Mechatronics (AIM'05), Monterey, CA, July 24–28.

Y. Hong is with the School of Mechanical Engineering, Purdue University, West Lafayette, IN 47907 USA (e-mail: hong9@purdue.edu).

B. Yao is with the School of Mechanical Engineering, Purdue University, West Lafayette, IN 47907 USA, and also a Kuang-piu Professor at the State Key Laboratory of Fluid Power Transmission and Control, Zhejiang University, Hangzhou 310027, China (e-mail: byao@purdue.edu).

Digital Object Identifier 10.1109/TMECH.2007.892835

measurement resolution) under nominal working condition. Furthermore, the projection-type adaptation of ARC can alleviate integral windup problem caused by parameter adaptations [10]. However, the previous ARC strategy [9], [13] does not guarantee global stability in the presence of actuator saturation. Specifically, the position feedback functions as an integral feedback for velocity loop that is immediately affected by the control input. Conventional ARC [9], [13] does not deal with the control saturation problem caused by large position tracking error (loosely speaking, one can think it as an integral windup problem for velocity feedback loop), as opposed to what the proposed controller in this paper is able to handle.

Essentially, a bounded virtual control law is designed to ensure the boundedness and convergence of the error signal at each step. The actual control input comes from the design at the final step, which consists of a model compensation term whose bound is calculable due to the preknown information of the system and the desired trajectory to be tracked, and a local-high-gain-but-globally-saturated robust control term to meet the dual objective of achieving global stability with limited control efforts for rare emergency cases and the local high-bandwidth control for high performance under normal running conditions. To better illustrate the essential idea and the high-performance nature of the proposed saturated ARC control strategy in practical applications, the precision control of a positioning system driven by linear motors [13] is considered. The same set of equipment has also been used to test the saturated ARC design in [7]. However, unlike in [7], the proposed saturated ARC design is based on the actual system states, in which state equations do not have model uncertainties except the last one since model uncertainties of these systems [13] are matched. As such, there is no need to consider the effect of model uncertainties until the final step of the design, removing the design conservativeness of [7]. Furthermore, the clear physical meaning of the actual system states makes it easier and more straightforward to select and tune the controller design parameters in implementation. All these make the proposed saturated ARC controller a more practical solution to the saturated actuator problem while without losing high performance under normal running conditions. Experimental results will be provided to illustrate these claims.

## II. Problem Formulation and Practical Assumptions

The linear motor used as a case study is a current-controlled three-phase epoxy core motor, which drives a linear positioning stage supported by recirculating bearings. Let $x_1$ and $x_2$ represent the stage position and velocity, respectively, and $x = [x_1, x_2]^T$ be the state vector. In order to capture the essential dynamics, the system model includes both viscous and Coulomb friction, the latter of which has a highly nonlinear effect approximated by the function $F_{sc}S_f(x_2)$ as in [13]; $F_{sc}$ represents the magnitude and $S_f(x_2)$ is a nondecreasing continuous function that approximates the discontinuous sign function $\mathrm{sgn}(x_2)$ that is normally used in the modeling of Coulomb friction. The governing equation is, thus, given by [13]

$$\begin{aligned} \dot{x}_1 &= x_2 \\ M\dot{x}_2 &= -Bx_2 - F_{sc}S_f(x_2) + d(t) + K_f u \end{aligned} \tag{1}$$

where $M$ is the inertia of the payload plus the coil assembly, $u$ is the control voltage with an input gain of $K_f, B$ and $F_{sc}$ represent the two major friction coefficients, viscous and Coulomb, respectively, and $d(t)$ represents the lumped external disturbances and unmodeled dynamics such as the nonlinear friction modeling errors and electromagnetic cogging and ripple forces of linear motors.

The aforementioned system is subject to unknown parameters due to payload variation $M$, uncertain friction coefficients $B$ and $F_{sc}$, the lumped neglected model dynamics and external disturbances $d(t)$, and the motor constant $K_f$. In principle, the algorithm proposed in this paper can be extended to the case where all these parameters are unknown without much theoretical difficulty. However, doing that will make the subsequent development rather complicated in terms of mathematical notations. As this paper mainly focuses on the essence of how to deal with input saturation in guaranteeing global stability while achieving excellent tracking performance under normal situations, the mass term $M$ and the motor constant $K_f$ are assumed to be known to simplify the derivations without losing generality and practical significance; compared to other parameters, these two parameters are unlikely to change during a single operation and can normally be estimated accurately online. With these simplifications, the aforementioned governing equations can be rewritten as

$$\begin{aligned} \dot{x}_1 &= x_2 \\ \dot{x}_2 &= -B_m x_2 - F_{scm}S_f(x_2) + d_{0m} + \Delta + \frac{K_f}{M}u \\ &= \varphi^T(x)\theta + \Delta + \overline{u} \end{aligned} \tag{2}$$

where $\varphi(x) = [-x_2, -S_f(x_2), 1]^T$ is the regressor, $\theta = [B_m, F_{scm}, d_{0m}]^T = [B, F_{sc}, d_0]^T/M$ is the vector of unknown parameters to be adapted on-line, $d_{0m}$ represents the nominal value of the normalized lumped uncertainties $d_m(t) = d(t)/M, \Delta = d_m(t) - d_{0m}$ represents the variation or high-frequency components of $d_m(t)$, and $\overline{u} = K_f u/M$ is the normalized control input whose upper and lower limits can be calculated from the physical input saturation level.

The following nomenclature is used throughout the paper: $\hat{\bullet}$ is used to denote the estimate of $\bullet$, $\tilde{\bullet}$ is used to denote the parameter estimation error of $\bullet$, e.g., $\tilde{\theta} = \hat{\theta} - \theta$, $\bullet_i$ is the $i$th component of the vector $\bullet$, $\bullet_{\max}$ and $\bullet_{\min}$ are the maximum and minimum value of $\bullet(t)$ for all $t$, respectively. The following practical assumptions are made for the system, which could be regarded as given information.

*Assumption 1:* The extents of the parametric uncertainties are known, i.e.,

$$B_m \in [B_{ml}, B_{mu}], F_{scm} \in [F_{scml}, F_{scmu}]$$

where $B_{ml}, B_{mu}, F_{scml}$, and $F_{scmu}$ are known.

For any controller to be able to stabilize the system even locally, the actuator has to be physically powerful enough to withstand the external disturbances. As such, only bounded disturbances will be considered, which leads to the following assumption.

*Assumption 2:* The lumped disturbance $d_m(t)$ is bounded, i.e.,

$$|d_m(t)| \leq \delta_{dm}$$

where $\delta_{dm}$ is known.

With the aforementioned assumptions, it is obvious that the parameter vector $\theta$ belongs to a set $\Omega_\theta$ as $\theta \in \Omega_\theta = \{\theta_{\min} \leq \theta \leq \theta_{\max}\}$, where $\theta_{\min} = [B_{ml}, F_{scml}, -\delta_{dm}]^T$, $\theta_{\max} = [B_{mu}, F_{scmu}, \delta_{dm}]^T$; the operation $\leq$ for two vectors is performed componentwise in this paper. The desired position $x_{1d}(t)$, velocity $x_{2d}(t) = \dot{x}_{1d}(t)$, and acceleration $\ddot{x}_{1d}(t)$ are assumed to be known and bounded. Let $\overline{u}_{bd}$ represent the normalized bound of the actuator authority. The saturation control problem can be stated as follows: *under the aforementioned assumptions and the normalized input constraint of* $|\overline{u}(t)| \leq \overline{u}_{bd}$, *design a control law that globally stabilizes the system and makes the output tracking error* $z_1 = x_1 - x_{1d}(t)$ *as small as possible*.

## III. Saturated Adaptive Robust Control

In this section, a saturated adaptive robust controller (ARC) will be presented to solve the aforementioned saturated control problem while pushing the achievable practical control performance to the limit.

### A. Saturated ARC Controller Design

The proposed saturated ARC design follows the standard backstepping design procedure [12] as follows.

From (1), $\dot{z}_1 = x_2 - \dot{x}_{1d}(t)$. The first step is to synthesize a bounded virtual control law $\alpha_1$ for $x_2$, so that the output tracking error $z_1$ converges to zero globally when $x_2 = \alpha_1$. For this purpose, denoting the actual input discrepancy as $z_2 = x_2 - \alpha_1$, then $z_1$ dynamics becomes

$$\dot{z}_1 = z_2 + \alpha_1 - \dot{x}_{1d}. \tag{3}$$

The saturated adaptive robust control (SARC) law for $\alpha_1$ is proposed as

$$\alpha_1 = \alpha_{1a} + \alpha_{1s}, \quad \alpha_{1a} = \dot{x}_{1d}, \quad \alpha_{1s} = -\sigma_1(z_1) \tag{4}$$

where $\sigma_1(z_1)$ is designed to be a smooth (first-order differentiable), nondecreasing, saturation function with respect to $z_1$ and it has the following four properties:

i) If $|z_1| < L_{11}$, then $\sigma_1(z_1) = k_1 z_1$.
ii) $z_1\sigma_1 > 0$, $\forall z_1 \neq 0$.
iii) $|\sigma_1(z_1)| \leq M_1, \forall z_1 \in \mathbb{R}$.
iv) $\left|\frac{\partial \sigma_1}{\partial z_1}\right| \leq k_1$, if $|z_1| < L_{12}$, and $\left|\frac{\partial \sigma_1}{\partial z_1}\right| = 0$, if $|z_1| \geq L_{12}$.

Graphically, such a saturation function can be drawn as in Fig. 1 and $L_{11}, L_{12}, k_1$, and $M_1$ are the positive design parameters to be specified in detail later.

With (4), (3) becomes

$$\dot{z}_1 = z_2 - \sigma_1(z_1) \tag{5}$$

which guarantees $z_1 \longrightarrow 0$ globally when $z_2 = 0$. So let us look at the dynamics of $z_2$:

$$\dot{z}_2 = \dot{x}_2 - \dot{\alpha}_1 = \varphi^T(x)\theta + \Delta + \overline{u} - \ddot{x}_{1d} + \frac{\partial \sigma_1}{\partial z_1}(z_2 - \sigma_1). \tag{6}$$

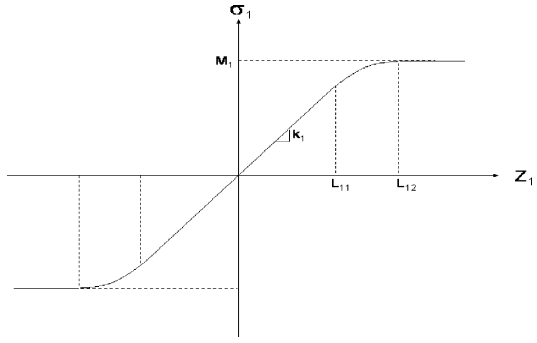


Fig. 1. Saturated robust control term for $z_1$.

Let $\overline{u} = \overline{u}_a + \overline{u}_s$ in which $\overline{u}_a$ represents the model compensation and $\overline{u}_s$ for robust term. The idea is to use $\overline{u}_a$ to compensate for the known part of the model dynamics for perfect tracking and $\overline{u}_s$ to fight against various model uncertainties including external disturbances. In addition, both $\overline{u}_a$ and $\overline{u}_s$ should be designed to be bounded to make sure that $\overline{u}$ stays within its saturation limits. The details are given later.

If the standard direct ARC designs [8], [13] were to be used, the model compensation $\overline{u}_a$ would be

$$\overline{u}_a = -\varphi^T(x)\hat{\theta} + \ddot{x}_{1d} + \frac{\partial \sigma_1}{\partial z_1}\sigma_1 \tag{7}$$

in which the parameter estimate $\hat{\theta}$ is to be updated on-line through a projection-type parameter estimation algorithm given by

$$\dot{\hat{\theta}} = \mathrm{Proj}_{\hat{\theta}}(\Gamma\tau), \quad \hat{\theta}(0) \in \Omega_\theta \tag{8}$$

where $\tau$ is the adaptation function to be synthesized later and the projection mapping is defined by

$$\mathrm{Proj}_{\hat{\theta}}(\bullet_i) = \begin{cases} 0, & \text{if } \hat{\theta}_i = \theta_{i\,\max} \text{ and } \bullet_i > 0 \\ 0, & \text{if } \hat{\theta}_i = \theta_{i\,\min} \text{ and } \bullet_i < 0 \\ \bullet_i, & \text{otherwise} \end{cases} \tag{9}$$

where $\Gamma$ is a diagonal matrix of adaptation rates. With the projection-type parameter estimation law (8), the parameter estimates $\hat{\theta}(t)$ always stay within their known bounds, i.e., $\theta_{\min} \leq \hat{\theta}(t) \leq \theta_{\max}, \forall t$. Thus, the parameter estimation errors $\tilde{\theta}(t) = \hat{\theta}(t) - \theta$ are always bounded with known bounds by $|\tilde{\theta}(t)| \leq \theta_{\max} - \theta_{\min}, \forall t$. In other words, such a parameter adaptation law has the following properties:

(P1) The parameter estimates are always within the known bound at any time instant $t$.
(P2) $\tilde{\theta}^T(\Gamma^{-1}\mathrm{Proj}_{\hat{\theta}}(\Gamma\tau) - \tau) \leq 0$.

As mentioned earlier, $\overline{u}_a$ needs to be bounded to enforce the essence of this saturated control design. However, the model compensation term by (7) contains $\varphi(x) = [-x_2, -S_f(x_2), 1]^T$, which obviously cannot be assumed bounded due to the appearance of $x_2$. Note that, $\varphi(x)$ can be rewritten as $[-z_2, 0, 0]^T + [-\alpha_1, -S_f(x_2), 1]^T$, where the

first term would go unbounded under a sudden and strong disturbance. Fortunately, it also acts as a damping to help stabilize the system. The second term, defined as $\varphi_b(x)$ (i.e., $\varphi_b(x) = [-\alpha_1, -S_f(x_2), 1]^T$) is always bounded. Overall, the parameter estimation law remains the same with the adaptation function being $\tau = \varphi_b(x)z_2$, whereas the bounded $\overline{u}_a$ is redesigned as follows:

$$\begin{aligned}\overline{u}_a &= \hat{B}_m\alpha_1 - [-S_f(x_2), 1] \cdot [\hat{F}_{scm}, \hat{d}_m]^T + \ddot{x}_{1d} + \frac{\partial\sigma_1}{\partial z_1}\sigma_1 \\ &= -\varphi_b^T(x)\hat{\theta} + \ddot{x}_{1d} + \frac{\partial\sigma_1}{\partial z_1}\sigma_1. \end{aligned} \tag{10}$$

The upper bound of $|\overline{u}_a|$, denoted as $\overline{u}_{abd}$, is easy to estimate according to property (P1), known desired trajectory and properties (iii) and (iv) of $\sigma_1$. Obviously, for the desired trajectory to be physically trackable, $\overline{u}_{abd}$ has to be less than the available control authority, i.e., $|\overline{u}_a| \le \overline{u}_{abd} < \overline{u}_{bd}$.

Apply the model compensation $\overline{u}_a$ in (10) and $z_2$ dynamics (6) becomes

$$\dot{z}_2 = -B_m z_2 - \varphi_b^T\tilde{\theta} + \Delta + \overline{u}_s + \frac{\partial\sigma_1}{\partial z_1}z_2. \tag{11}$$

Based on the boundedness of $\varphi_b$ and Assumption 2, it can be assumed that $|-\varphi_b^T(x)\tilde{\theta} + \Delta| \le h$, where $h$ could be regarded as the bound of the total effect of model mismatch plus the unmodeled uncertainties under the normal working condition and estimated according to the prior known information.

As can be seen from (11), the robust term $\overline{u}_s$ needs to overcome the term coming from the first channel $(\partial\sigma_1/\partial z_1)z_2$ plus the bounded model mismatch in order to make $z_2$ converge or, at least, bounded.

In order to actively take into account the actuator saturation problem when the control law is designed, another nondecreasing function $\sigma_2(z_2)$ is used to construct $\overline{u}_s$. Let $\overline{u}_s = -\sigma_2(z_2)$, where $\sigma_2(z_2)$ has the following properties:

i) $\forall z_2 \in \{z_2 : |z_2| < L_{21}\}, \sigma_2(z_2) = k_{21}z_2$.
ii) $\forall z_2 \in \{z_2 : L_{21} \le |z_2| \le L_{22}\}, \frac{\partial\sigma_2}{\partial z_2} \ge k_{21}, \sigma_2(L_{22}) = M_2$ and $\sigma_2(-L_{22}) = -M_2$.
iii) $\forall z_2 \in \{z_2 : |z_2| > L_{22}\}, |\sigma_2(z_2)| \ge M_2$.

Notice this is the last channel of the system and $\overline{u}_s$ is a part of the real control input, therefore, $\sigma_2(z_2)$ only needs to be continuous instead of smooth. Fig. 2 shows an example of $\sigma_2(z_2)$ that has all the required properties. The design parameters are $L_{21}, k_{21}, L_{22}$, and $k_{22}$. The complete form of control input is, thus, as follows:

$$\overline{u} = -\varphi_b^T\hat{\theta} + \ddot{x}_{1d} + \frac{\partial\sigma_1}{\partial z_1}\sigma_1 - \sigma_2(z_2). \tag{12}$$

*Remark 1:* Notice that $\sigma_2(z_2)$ has two regions with different gains whereas $\sigma_1(z_1)$ has only one linear gain. This is due to the fact that the model mismatch and uncertainties only appear in $z_2$ dynamics. The region with moderate gain $k_{21}$ represents the normal operation of the system and is selected to achieve high performance such as short transient periods and small tracking errors while remaining insensitive to noise effects. When $|z_2|$ is between $L_{21}$ and $L_{22}$, for example, during the transient period or when model mismatch is large, more aggressive gain $k_{22}$ is employed to reduce transient tracking error and to improve the disturbance rejection. This high-gain $k_{22}$ could also be designed as a certain nonlinear function to achieve further improvement. When some emergences happen, such as an overpowering random strike on the positioning stage that drags system states far away from the normal operation region, i.e., $|z_2| \gg L_{22}, \sigma_2$ is a constant, so that the overall control effort is always guaranteed to stay within the physical limit of the actuator. When the huge disturbance is gone, the proposed control strategy can pull the state back to the nominal working range and regain high performance as proved in the following subsection.

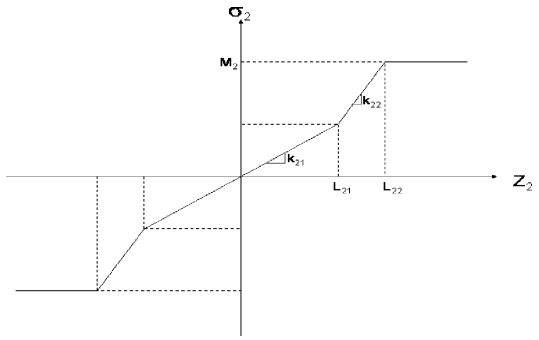


Fig. 2. Saturated robust control term for $z_2$.

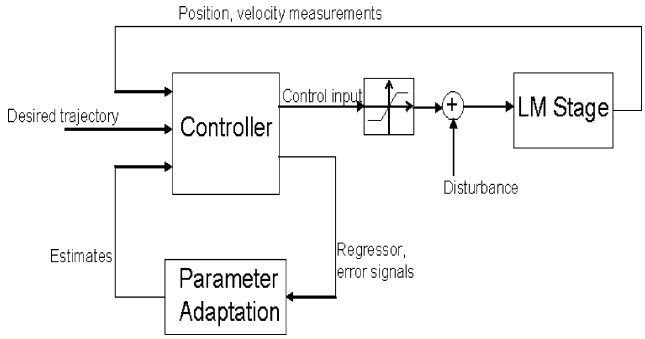


Fig. 3. Design structure.

In summary, the overall design structure is illustrated as Fig. 3

### B. Proof of Globally Stability and Asymptotic Tracking

By combining (5) and (11), the error dynamics can be rewritten as follows:

$$\begin{aligned}\dot{z}_1 &= z_2 - \sigma_1(z_1) \\ \dot{z}_2 &= -B_m z_2 - \varphi_b^T(x)\tilde{\theta} + \Delta + \frac{\partial\sigma_1}{\partial z_1}z_2 - \sigma_2(z_2). \end{aligned} \tag{13}$$

Before the evolutions of $z_1$ and $z_2$ are analyzed in details, the following constraints on the controller design parameters are enforced in order to guarantee the global stability of the controlled system: (a) $k_{21} > k_1$, (b) $k_1 L_{11} > L_{22}$,

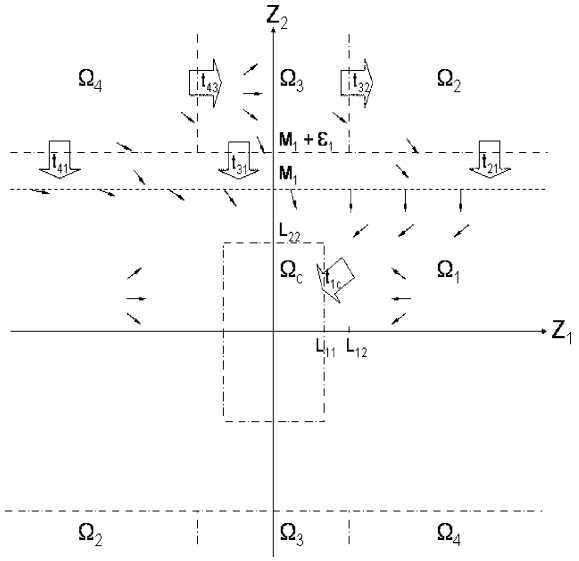


Fig. 4. $z_1$–$z_2$ plane.

(c) $M_2 > h + k_1 M_1$, and (d) $M_2 \leq \overline{u}_{bd} - \overline{u}_{abd}$. The essential idea to guarantee the global stability of such a system is to divide the plane into four regions and analyze the error dynamics in each region. The conclusion is that no matter where the initial state starts, the trajectory will converge to a preset region $\Omega_c = \{z_1, z_2 : |z_1| \leq L_{11}, |z_2| \leq L_{22}\}$ in finite time with the upper bound of the convergence time estimated accordingly.

*Remark 2:* Constraints (a)–(d) are the minimum requirements that the control parameters have to satisfy in order to make the system globally stable. Further research can be done to explore the flexibility of choosing controller parameters given the aforementioned constraints to optimize the achievable performance.

*Theorem 1: With the proposed controller (4) with (12) satisfying conditions (a)–(d), all signals are bounded. Furthermore, the error state $[z_1, z_2]^T$ reaches the preset region $\Omega_c$ in a finite time and stay within thereafter. At steady state, the final tracking error is bounded above by $|z_1(\infty)| \leq h/[k_1(k_{21} - k_1)]$.*

*Proof:* Due to the special properties of the saturation function designed for $\sigma_1$ and $\sigma_2$, it is convenient to carry out the proof by dividing the $z_1$–$z_2$ plane into several regions and analyzing the traveling time from one region to another. As a result, the upper bound of the reaching time from any arbitrary initial condition to the convergence region could be estimated.

With conditions (b) and (c), there exist positive $\epsilon_1, \epsilon_2$, and $\epsilon_3$, such that $L_{22} + \epsilon_3 < k_1 L_{11}$ and $h + k_1(M_1 + \epsilon_1) + \epsilon_2 < M_2$. Noting $M_1 > k_1 L_{11} > L_{22}$, as shown in Fig. 4, the entire $z_1$–$z_2$ plane is divided into four regions $\Omega_1$–$\Omega_4$ defined as follows:

$$\Omega_c = \{z : |z_1| \leq L_{11}, |z_2| \leq L_{22}\}$$
$$\Omega_1 = \{z : |z_2| \leq M_1 + \epsilon_1\}$$
$$\Omega_2 = \{z : z_2(z_1 - \text{sign}(z_2)L_{12}) > 0, |z_2| > M_1 + \epsilon_1\}$$
$$\Omega_3 = \{z : |z_1| \leq L_{12}, |z_2| > M_1 + \epsilon_1\}$$
$$\Omega_4 = \{z : z_2(z_1 + \text{sign}(z_2)L_{12}) < 0, |z_2| > M_1 + \epsilon_1\}.$$

Notice that $\Omega_c \subset \Omega_1$. In the following procedures, four claims will be stated and proved, which leads to the final conclusion of the global stability.

*Claim 1:* Any trajectory starting from $\Omega_1$ will enter $\Omega_c$ in a finite time $t_{1c}$ and stay within thereafter.

*Proof:* Consider the trajectory with the state satisfying $L_{22} \leq |z_2(t)| \leq M_1 + \epsilon_1$ first. Then, noting the properties of $\sigma_1(z_1)$ and $\sigma_2(z_2)$, the following inequality can be established according to the error dynamics (13):

$$\begin{aligned} z_2 \dot{z}_2 &\leq |z_2|(h - B_m|z_2| + k_1|z_2| - |\sigma_2(z_2)|) \\ &\leq |z_2|(h + k_1(M_1 + \epsilon_1) - M_2) \\ &\leq -\epsilon_2|z_2| \end{aligned} \tag{14}$$

which indicates that any trajectory starting with an initial state of $L_{22} \leq |z_2(0)| \leq M_1 + \epsilon_1$ will reach the region $\Omega_5 = \{z : |z_2(t)| \leq L_{22}\}$ in a finite time $t_{1c,2}$ and stay within $\Omega_5$ thereafter. Furthermore, the upper bound of the reaching time $t_{1c,2}$ is

$$t_{1c,2} \leq \max\left\{0, \frac{|z_2(0)| - L_{22}}{\epsilon_2}\right\}. \tag{15}$$

Within the region $\Omega_5$, i.e., $|z_2(t)| \leq L_{22}$, if $|z_1(t)| > L_{11}$, from (13) and properties (i) and (ii) of the nondecreasing function $\sigma_1(z_1)$,

$$\begin{aligned} z_1 \dot{z}_1 &\leq |z_1|(L_{22} - |\sigma_1(z_1)|) \\ &\leq |z_1|(L_{22} - k_1 L_{11}) \leq -\epsilon_3|z_1|. \end{aligned} \tag{16}$$

Thus, any trajectory starting within $\Omega_5$ with $|z_1(0)| > L_{11}$ will reach the region $\Omega_c$ in a finite time $t_{1c,1}$ and stay within $\Omega_c$ thereafter. Furthermore, the upper bound of the reaching time $t_{1c,1}$ can be obtained from (16) as

$$t_{1c,1} \leq \max\left\{0, \frac{|z_1(t_{1c,2})| - L_{11}}{\epsilon_3}\right\}. \tag{17}$$

By combining (15) and (17), the upper bound of the reaching time for the trajectory starting within $\Omega_1$ to $\Omega_c$ is obtained

$$\begin{aligned} t_{1c} &= t_{1c,2} + t_{1c,1} \\ &\leq \max\left\{0, \frac{|z_2(0)| - L_{22}}{\epsilon_2}\right\} + \max\left\{0, \frac{|z_1(t_{1c,2})| - L_{11}}{\epsilon_3}\right\}. \end{aligned} \tag{18}$$

*Claim 2:* Any trajectory starting from $\Omega_2$ will enter $\Omega_1$ in a finite time $t_{21}$.

*Proof:* In $\Omega_2, z_1 z_2 > 0, |z_1| > L_{12}$, and $|z_2| > M_1 + \epsilon_1 > L_{22}$. From property (iv) of $\sigma_1, \partial\sigma_1/\partial z_1 = 0$; from property (iii) of $\sigma_2, |\sigma_2| \geq M_2$. Thus, from (13), noting property (iii) of $\sigma_1$

$$\begin{aligned} z_1 \dot{z}_1 &\geq |z_1|(M_1 + \epsilon_1 - M_1) \geq \epsilon_1|z_1| \\ z_2 \dot{z}_2 &\leq |z_2|(h - (B_m)|z_2| - M_2) \leq -(M_2 - h)|z_2| \end{aligned} \tag{19}$$

which implies that in $\Omega_2, |z_1(t)|$ will increase but $|z_2(t)|$ will strictly decrease to $M_1 + \epsilon_1$. Therefore, any trajectory starting within $\Omega_2$ will reach $\Omega_1$ in a finite time $t_{21}$. The upper bound of

the reaching time $t_{21}$ can be obtained from (19) as

$$t_{21} \leq \frac{|z_2(0)| - (M_1 + \epsilon_1)}{M_2 - h}. \tag{20}$$

*Claim 3:* Any trajectory starting from $\Omega_3$ will enter either $\Omega_1$ in a finite time $t_{31}$ or $\Omega_2$ in a finite time $t_{32}$.

*Proof:* In $\Omega_3, |z_1| \leq L_{12}$ and $|z_2| > M_1 + \epsilon_1$. According to property (iii) of $\sigma_1, |\sigma_1| \leq M_1$. From (13), when $z_2 \geq M_1 + \epsilon_1$,

$$\dot{z}_1 = z_2 - \sigma_1 \geq M_1 + \epsilon_1 - M_1 \geq \epsilon_1 \tag{21}$$

and when $z_2 \leq -(M_1 + \epsilon_1)$,

$$\dot{z}_1 = z_2 - \sigma_1 \leq -(M_1 + \epsilon_1) + M_1 \leq -\epsilon_1. \tag{22}$$

Equations (21) and (22) imply that, for any trajectory starting from $\Omega_3$, if it does not enter $\Omega_1$, it will enter $\Omega_2$ in a finite time $t_{32}$. The upper bound of the reaching time $t_{32}$ can be obtained as

$$t_{32} \leq \frac{|L_{12}\,\mathrm{sign}(z_2) - z_1(0)|}{\epsilon_1}. \tag{23}$$

It is also possible that the trajectory will enter $\Omega_1$ within a finite time $t_{31}$. If that happens, the reaching time $t_{31}$ should be smaller than the one obtained in (23), i.e., $t_{31} \leq t_{32} \leq |L_{12}\,\mathrm{sign}(z_2) - z_1(0)|/\epsilon_1$.

*Claim 4:* Any trajectory starting from $\Omega_4$ will enter either $\Omega_1$ in a finite time $t_{41}$ or $\Omega_3$ in a finite time $t_{43}$.

*Proof:* In $\Omega_4, z_1 z_2 < 0, |z_1| > L_{12}$, and $|z_2| > M_1 + \epsilon_1 > L_{22}$. Thus, from (13), when $z_2 \geq M_1 + \epsilon_1, z_1 < -L_{12}$ and $\sigma_1 = -M_1$

$$\dot{z}_1 = z_2 - \sigma_1 \geq M_1 + \epsilon_1 + M_1 \geq \epsilon_1 + 2M_1 \tag{24}$$

and when $z_2 \leq -(M_1 + \epsilon_1), z_1 > L_{12}$ and $\sigma_1 = M_1$

$$\dot{z}_1 = z_2 - \sigma_1 \leq -(M_1 + \epsilon_1) - M_1 \leq -(\epsilon_1 + 2M_1). \tag{25}$$

Thus, for any trajectory starting from $\Omega_4$, if it does not enter $\Omega_1$, it will enter $\Omega_3$ in a finite time $t_{43}$. The upper bound of the reaching time $t_{43}$ can be obtained as

$$t_{43} \leq \frac{|z_1(0)| - L_{12}}{2M_1 + \epsilon_1}. \tag{26}$$

It is also possible that the trajectory will enter $\Omega_1$ within a finite time $t_{41}$. If that happens, the reaching time $t_{41}$ should be smaller than the one obtained in (26), i.e., $t_{41} \leq t_{43} \leq (|z_1(0)| - L_{12})/(2M_1 + \epsilon_1)$. Another estimation of $t_{41}$ could be made as follows. From property (iv) of $\sigma_1$, $\partial\sigma_1/\partial z_1 = 0$; from property (iii) of $\sigma_2$, $z_2\sigma_2 \geq |z_2|M_2$,

$$z_2\dot{z}_2 \leq |z_2|(h - M_2), \quad t_{41} \leq \frac{|z_2(0)| - (M_1 + \epsilon_1)}{M_2 - h}. \tag{27}$$

In all, with Claims 1–4, no matter where the trajectory starts, it will enter $\Omega_c$ in a finite time and stay within thereafter. As shown in the upper half plane of Fig. 4, little black arrows represent the phase portrait and big hollow arrows indicate the state traveling from one region to another with the reaching time marked on. The global stability is, thus, proved.

Once the trajectory enters $\Omega_c = \{z : |z_1| \leq L_{11}, |z_2| \leq L_{22}\}$, the error dynamics become

$$\begin{aligned}\dot{z}_1 &= z_2 - k_1 z_1 \\ \dot{z}_2 &= (-\varphi_b^T\tilde{\theta} + \Delta) \\ &\quad + (-B_m + k_1)z_2 - \sigma_2(z_2).\end{aligned} \tag{28}$$

Define a positive semidefinite function $V_2 = z_2^2/2$ and let $k_s = k_{21} - k_1$. From the second equation of (28), the derivative of $V_2$ is given by

$$\begin{aligned}\dot{V}_2 &= z_2\dot{z}_2 \\ &\leq |z_2|(h + k_1|z_2| - k_{21}|z_2|) \\ &\leq -\frac{k_s}{2}z_2^2 + h|z_2| - \frac{k_s}{2}z_2^2 \\ &\leq -\frac{k_s}{2}(|z_2| - \frac{h}{k_s})^2 + \frac{h^2}{2k_s} - \frac{k_s}{2}z_2^2 \\ &\leq \frac{h^2}{2k_s} - \frac{k_s}{2}z_2^2 \\ &\leq -k_s V_2 + \frac{h^2}{2k_s}\end{aligned} \tag{29}$$

which leads to the following inequality:

$$V_2(t) \leq \exp(-k_s t)V_2(0) + \frac{h^2}{2k_s^2}[1 - \exp(-k_s t)]. \tag{30}$$

From (30), the steady state of $z_2$ is bounded by $|z_2(\infty)| \leq h/k_s$. Then, according to the first equation of (28), the steady-state tracking error $z_1$ is bounded by $|z_1(\infty)| \leq h/(k_1 k_s) = h/[k_1(k_{21} - k_1)]$, as stated in Theorem 1.

*Remark 3:* From this proof, it can be seen that every constraint on the control parameters has its practical meaning. Constraint (a) requires the gains in the second channel to be greater than $k_1$ in order to overpower the term $\partial\sigma_1/\partial z_1$ in $z_2$ dynamics (13). Constraint (b) guarantees that once $z_2$ is bounded within a preset range, $z_1$ is ensured to decrease and be bounded accordingly. Constraint (c) implies that, for the design problem to be meaningful, the level of lumped modeling error and disturbance should be within the limit of the control authority available for robust feedback. Constraint (d) implies that a tradeoff has to be made between the amount of model uncertainties to which the system can be made robust, and the aggressiveness of the trajectory that it can follow (i.e., the larger the bound $h$ becomes, the larger $M_2$ is needed for robust feedback; whereas a more aggressive desired trajectory leads to a larger bound $\overline{u}_{abd}$ of the model compensation). Overall, these constraints are easy to meet practically and are favorably posed to attain global stability as well as good local performance. To be more specific, theoretically, there is no absolute restriction on how large the feedback gains $(k_1, k_{21}, k_{22})$ can be. This means the steady-state tracking error can be made arbitrarily small, as seen from Theorem 1. In terms of robustness, the controlled system can tolerate a large class of modeling error and external disturbances, even those with a magnitude close to $M_2$. Whereas in [7], significant conservativeness exists in this matter.

Now that it is proved that all signals are bounded after finite time, the remainder of this section is to demonstrate that asymptotic tracking is achievable in the presence of parameter estimation error only, i.e., $\Delta = 0$.

*Theorem 2: With the proposed controller (4) and (12) satisfying conditions (a)–(d) and the adaptation law (8) and (9), asymptotic output tracking is achieved if the system is only subject to parametric uncertainty after a finite time, i.e.,* $\Delta = 0, \forall t \geq t_0$ for some $t_0$.

*Proof:* Introduce a positive semidefinite function $V_a = (1/2)z_2^2 + (1/2)\tilde{\theta}^T\Gamma^{-1}\tilde{\theta}$. In the case of $\Delta = 0$, with property 2 of the parameter estimation law, $\dot{V}_a$ becomes

$$\begin{aligned}\dot{V}_a &= z_2\dot{z}_2 + \tilde{\theta}^T\Gamma^{-1}\dot{\tilde{\theta}} \\ &= z_2\left(-B_m z_2 - \varphi_b^T(x)\tilde{\theta} + \frac{\partial\sigma_1}{\partial z_1}z_2 - \sigma_2(z_2)\right) \\ &\quad + \tilde{\theta}^T\Gamma^{-1}\mathrm{Proj}_{\hat{\theta}}(\Gamma\varphi_b z_2) \\ &\leq -B_m z_2^2 - \left(z_2\sigma_2(z_2) - \frac{\partial\sigma_1}{\partial z_1}z_2^2\right) \qquad (31)\end{aligned}$$

which is negative semidefinite once $z_1$ and $z_2$ evolve to $\Omega_c$ as proved. As a result, $z_2$ converges to zero asymptotically and so would $z_1$ according to (5). Hence, asymptotic output tracking is achieved.

## IV. Hardware Experiments

### A. System Setup

The linear motor system under study is described in detail in [13]. The control algorithm is designed and tested on the Y-axis of the stage. The current loop of the amplifier has the bandwidth as high as 2 kHz; therefore, its dynamics is neglected. The mass of the stage and coil assembly is 3.34 kg and the input gain $K_f$ is 27.79. The bound $\overline{u}_{bd}$ is 83.2 corresponding to the physical input voltage limit of 10 V. The sampling frequency is 2.5 kHz. The resolution of the position sensor is 1 $\mu$m and the feedback velocity signal is obtained by conducting "backward difference" of the position feedback.

### B. Implementation Issue and Design Parameters

When implementing the designed control law in real-time experiments, a modification on function $\sigma_2$ shown in Fig. 2 is used to further improve the performance. Specifically, the example $\sigma_2$ in Fig. 2 has a constant control effort when $|z_2| > L_{22}$. Considering the fact that the actual amount of control effort for the model compensation $\overline{u}_a$ during most of the running period is smaller than the estimated upper bound $\overline{u}_{abd}$, the total actuator effort $\overline{u}$ may not be in its physical limit to put in all available power to attenuate the disturbance even though the robust control term reaches its maximum value. To improve the system's ability to cope with large disturbances, the magnitude restriction on function $\sigma_2$ is removed so that $\sigma_2$ keeps increasing monotonically and the physical actuator becomes saturated naturally. Such a $\sigma_2$ still satisfies properties (i)–(iii) and, thus, the overall system's global stability is guaranteed.

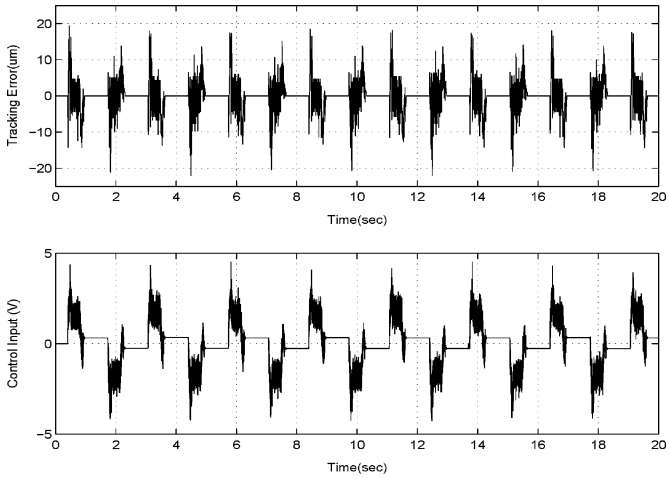


Fig. 5. Tracking error and control input (without disturbance).

The control parameters are selected as follows: $L_{11} = 50\,\mu$m, $L_{12} = 70\,\mu$m, $k_1 = 500, M_1 = 1.2k_1L_{11}, L_{21} = 0.5M_1, k_{21} = k_1 + 600, k_{22} = k_{21} + 200, M_2 = 0.99\,(\overline{u}_{bd} - \overline{u}_{abd})$, $L_{22} = (M_{22} - k_{21}L_{21})/k_{22} + L_{21}$. As long as the design parameters satisfy constraints (a)–(d), global stability is guaranteed. As to the tracking performance and closed-loop bandwidth, each system has its own physical limitation and sensor noise; thus, control parameters should be designed accordingly.

### C. Real-Time Experimental Results

Two sets of desired trajectories are designed to illustrate the effectiveness of the proposed control law. The point-to-point trajectory duplicates the regular maneuver in the manufacturing industry, while the step trajectory represents the extreme case for the linear motor to track.

*1) Point-To-Point Trajectory:* The point-to-point trajectory is at least second-order differentiable (meaning the acceleration being continuous), with a distance of 0.4 m, a maximum velocity of 1 m/s, and a maximum acceleration of 12 m/s$^2$, which is the same reference trajectory as in [13].

The experimental results with the proposed saturated ARC are given in Figs. 5 and 6. It can be seen that the position error converges quickly in Fig. 5 and the steady-state error is within 1 $\mu$m. Both transient and steady-state performances could be improved by employing a better parameter estimation algorithm such as recursive least square method [12].

Fig. 6 shows the tracking error and control effort under a 1 V constant disturbance added to the physical control input $u$. It is about 10% of the total control authority, which represents the normal working environment. With the Matlab program, the disturbance is introduced to the system at 3 s and lasts 10 s. As can be seen from the plot, the system adjusts well and the tracking error remains at the same level as it is in Fig. 5 due to the parameter adaptation mechanism. The parameter estimates are not shown here because the estimation law is of direct type that normally does not lead to accurate estimates of individual parameters [11].

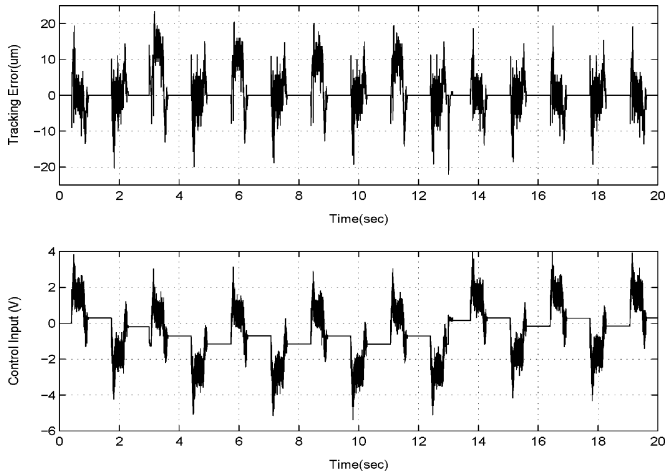


Fig. 6. Tracking error and control input (with 1-V disturbance).

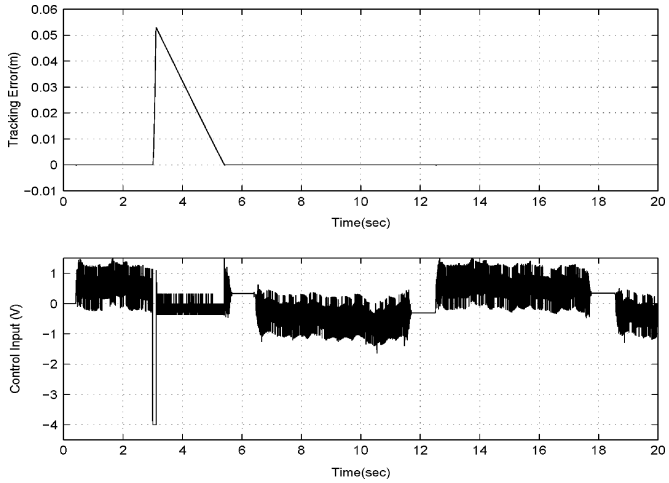


Fig. 7. Tracking error and control input (with 6-V disturbance).

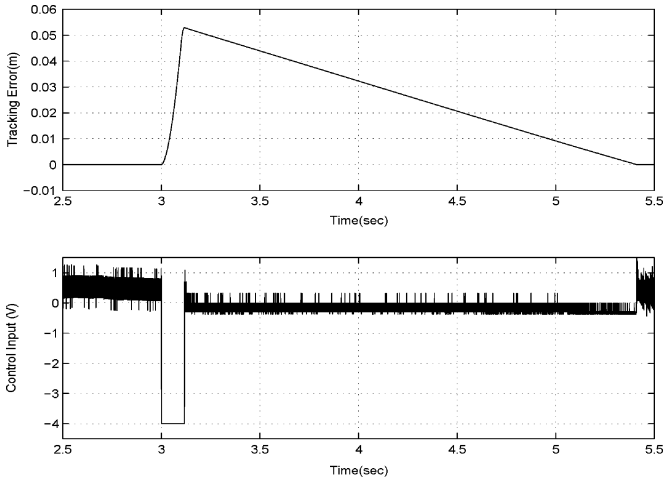


Fig. 8. Tracking error and control input (in the presence of 6-V disturbance).

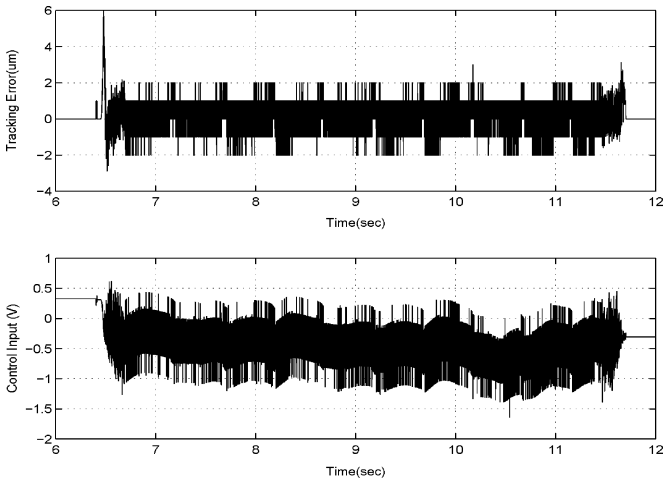


Fig. 9. Tracking error and control input (zoomed-in portion at steady state).

To demonstrate the global stability of the proposed saturated controller, as well as how effectively the controlled system deals with the practical scenario of experiencing an accident, such as a strong but short disturbance, experiments are conducted as follows. The actual input limit of the hardware is 10 V, while the physical limit of the control input is purposely set at 4 V, so that a step input, with the amplitude of 6 V and a duration of 0.1 s, can be injected as a disturbance and implemented by the hardware. The desired trajectory is also changed to be less aggressive due to the reduced control input authority, with a distance of 0.1 m, a maximum velocity of 0.02 m/s, and a maximum acceleration of 0.1 m/s$^2$.

Experimental results are shown in Figs. 7–9. Fig. 7 provides an overall view of the tracking error and control input during the entire operation time. Fig. 8 emphasizes the time period when the strong input disturbance happens. As seen from the plots, when the strong input disturbance is inserted at 3 s, the control input is not sufficient to overpower the disturbance and it saturates at the 4-V limit level with the tracking error accumulating to over 0.05 m. After the strong input disturbance is removed 0.1 s later, the tracking error reduces to the encoder resolution level of 1 $\mu$m at steady state, as shown in Fig. 9.

The aforementioned results support the claim that the proposed saturated ARC can achieve high performance under normal working environment and ensure global stability in case of unexpected strong disturbances.

*2) Step Trajectory:* Normally, step signal is not a feasible trajectory for a physical system to track due to the infinite value of its derivative at the step instant. The system will have large initial error that would easily saturate the control input with high-gain feedback and cause potential instability. Therefore, certain trajectory planning between the initial point and the set point is necessary to avoid that problem. The point-to-point trajectory described in the previous section is an example of a feasible one. However, in a few industry applications such as the hard disk drive (HDD) servomechanism, point-to-point movement is frequent and random whereas trajectory planning is not convenient or economic to conduct. A common solution in HDD servomechanism is to switch the system between the "seeking mode" and the "tracking mode" when tracking a step reference. The proposed strategy provides an alternative

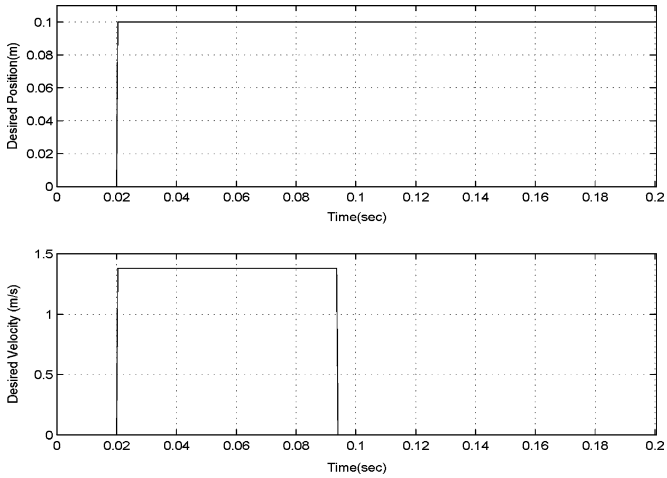


Fig. 10. Desired position and velocity trajectory (step reference).

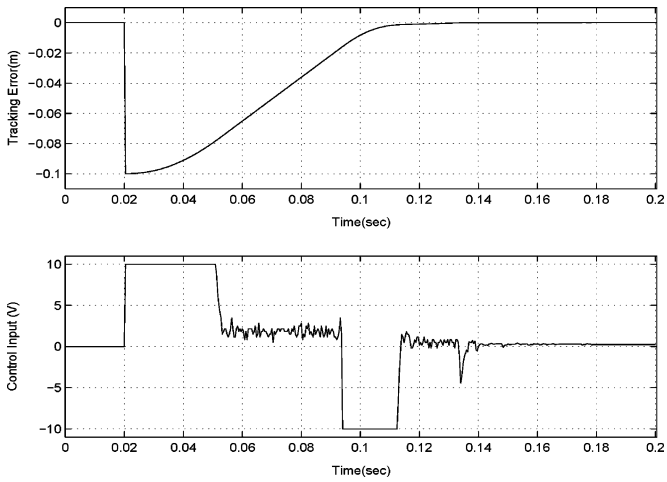


Fig. 11. Tracking error and control input (step reference).

to those methods as it could achieve good tracking performance and ensure stability with a built-in smooth "switching" controller.

In the hardware experiments, as shown in Fig. 10, the desired position trajectory for the linear motor is a step signal with the amplitude of 0.1 m. Since the controller has direct effect on the velocity, another step signal with the amplitude of 1.36 m/s (about the maximum velocity that the hardware can provide) is employed as the desired velocity trajectory and it steps down to zero 0.076 s later. The value 0.076 is estimated based on the desired trajectory, the maximum acceleration of the hardware and the control parameters, in order to obtain the minimum settling time of the controlled system. However, due to the modeling uncertainties of the linear motor system, this number does not guarantee the fastest tracking in real-time experiments, although it is good enough for the illustration purpose.

The experimental results with the step references are shown in Fig. 11, and Fig. 12 shows the zoomed-in portion at its steady

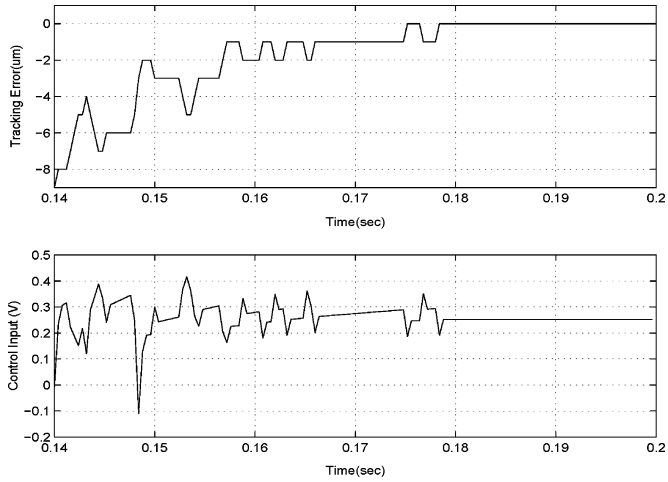


Fig. 12. Tracking error and control input at steady state (step reference).

state. As can be seen from Fig. 11, the actuator uses its maximum power $\pm 10$ V to speed up at the beginning and slow down when the stage is close to the 0.1 m set point. Between the acceleration and deceleration, the stage approaches to the set point at full speed. With this strategy, the controlled system can track the step reference with minimum time. Fig. 12 shows that the final tracking error is at the 1 $\mu$m resolution level and it enters the range of $\pm 10$ $\mu$m, 0.01% of the travel distance, after roughly 0.12 s.

## V. Conclusion

A saturated ARC algorithm was proposed to guarantee global stability and good tracking performance for the linear motor system that is subject to limited control authority, model uncertainties, and external disturbances. Such a goal was accomplished by taking the actuator saturation problem into account at the design stage and employing saturation function in the control algorithm. An identification law of projection type was applied to provide bounded parameter estimates and attain asymptotic tracking performance in the presence of parametric uncertainties only. Real-time experiments were presented to support the study.

## References

[1] D. S. Bernstein and A. N. Michel, "A chronological bibliography on saturating actuators," *Int. J. Robust Nonlinear Control*, vol. 5, pp. 375–380, 1995.

[2] H. J. Sussmann and Y. Yang, "On the stabilizability of multiple intergrators by means of bounded feedback controls," in *Proc. IEEE Conf. Decis. Control*, Brighton, U.K., 1991, pp. 70–72.

[3] A. Saberi, Z. Lin, and A. R. Teel, "Control of linear systems with saturating actuators," *IEEE Trans. Autom. Control*, vol. 41, no. 3, pp. 368–378, Mar. 1996.

[4] Z. Lin and A. Saberi, "A semi-global low-and-high gain design technique for linear systems with input saturation-stabilization and disturbance rejection," *Int. J. Robust Nonlinear Control*, vol. 5, pp. 381–398, 1995.

[5] A. R. Teel, "Linear systems with input nonlinearities: Global stabilization by scheduling a family of $H_\infty$ type controllers," *Int. J. Robust Nonlinear Control*, vol. 5, pp. 399–411, 1995.

[6] A. R. Teel, "Global stabilization and restricted tracking for multiple integrators with bounded controls," *Syst. Control Lett.*, vol. 18, pp. 165–171, 1992.

[7] J. Q. Gong and B. Yao, "Global stabilization of a class of uncertain systems with saturated adaptive robust control," in *Proc. IEEE Conf. Decis. Control*, Sydney, Australia, 2000, pp. 1882–1887.
[8] B. Yao and M. Tomizuka, "Adaptive robust control of SISO nonlinear systems in a semi-strict feedback form," *Automatica*, vol. 33, no. 5, pp. 893–900, 1997.
[9] B. Yao, "High performance adaptive robust control of nonlinear systems: A general framework and new schemes," in *Proc. IEEE Conf. Decis. Control*, San Diego, CA, 1997, pp. 2489–2494.
[10] B. Yao, M. Al-Majed, and M. Tomizuka, "High performance robust motion control of machine tools: An adaptive robust control approach and comparative experiments," *IEEE/ASME Trans. Mechatronics*, vol. 2, no. 2, pp. 63–76, Jun. 1997.
[11] B. Yao, "Integrated direct/indirect adaptive robust control of SISO nonlinear systems transformable to semi-strict feedback forms," in *Proc. Amer. Control Conf.*, 2003, pp. 3020–3025.
[12] M. Krstić, I. Kanellakopoulos, and P. Kokotovic, *Nonlinear and Adaptive Control Design*. New York: Wiley, 1995.
[13] L. Xu and B. Yao, "Adaptive robust precision motion control of linear motors with negligible electrical dynamics: Theory and experiments," *IEEE/ASME Trans. Mechatronics*, vol. 6, no. 4, pp. 444–452, Dec. 2001.

**Yun Hong** received the B.Eng. degree in automatic control from the University of Science and Technology of China, Hefei, China, in 2001. She subsequently joined the School of Mechanical Engineering, Purdue University, West Lafayette, IN, for her graduate study and was admitted to the direct Ph.D. program in 2002.

**Bin Yao** received the B.Eng. degree in applied mechanics from Beijing University of Aeronautics and Astronautics, Beijing, China, in 1987, the M.Eng. degree in electrical engineering from Nanyang Technological University, Singapore, in 1992, and the Ph.D. degree in mechanical engineering from the University of California, Berkeley, in 1996.

Since 1996, he has been with the School of Mechanical Engineering, Purdue University, West Lafayette, IN, where he became an Associate Professor in 2002. He is also one of the Kuang-piu Lecture Professors at Zhejiang University, Hangzhou, China, and a Guest Professor at Shenzhen Graduate School, Harbin Institute of Technology, Harbin, China. His current research interests include the design and control of intelligent high-performance coordinated control of electromechanical/hydraulic systems, optimal adaptive and robust control, nonlinear observer design and neural networks for virtual sensing, modeling, fault detection, diagnostics, and adaptive fault-tolerant control, and data fusion. He is the author or coauthor of more than 130 technical papers and enjoys the application of theory through industrial consulting.

Dr. Yao was awarded a Faculty Early Career Development (CAREER) Award by the National Science Foundation (NSF) in 1998 and a Joint Research Fund for Overseas Young Scholars from the National Natural Science Foundation of China (NSFC) in 2005. He was also the recipient of the O. Hugo Schuck Best Paper (Theory) Award from the American Automatic Control Council in 2004. He is a member of the American Society of Mechanical Engineers (ASME) and has chaired numerous sessions of the International Program Committees and served in a number of IEEE, ASME, and International Federation of Automatic Control (IFAC) conferences. From 2000 to 2002, he was the Chair of the Adaptive and Optimal Control Panel and, from 2001 to 2003, the Chair of the Fluid Control Panel of the ASME Dynamic Systems and Control Division (DSCD). He is currently the Vice-Chair of the ASME DSCD Mechatronics Technical Committee, which he initiated in 2005. From 2001 to 2005, he was a Technical Editor of the IEEE/ASME TRANSACTIONS ON MECHATRONICS, and since 2006, he has been an Associate Editor of the *ASME Journal of Dynamic Systems, Measurement, and Control*.